Proceedings of the 5th International
IEEE EMBS Conference on Neural Engineering
Cancun, Mexico, April 27 - May 1, 2011

Addressable Floating Light Activated Micro-Electrical Stimulators for Wireless Neurostimulation

David S. Freedman, Philipp S. Spuhler, Elif Cevik, M. Selim Unlu, *Fellow, IEEE*,
and Mesut Sahin, *Senior Member, IEEE*

***Abstract*— Stimulation of the central nervous system can be useful for treating neurological disorders. Wireless neurostimulating devices have the benefit that they can float in tissue and do not experience the sheering caused by tethering tension that non-wireless stimulators impose on connecting wires. An optically powered, logic controlled, CMOS microdevice that can decode telemetry data from an optical packet is a potential way of implementing wireless, addressable, microstimulators. Through the use of an optical packet, different devices can be addressed for stimulation, allowing spatially selective activation of neural tissue. This work presents the design and simulations of such a neural stimulation device, specifically an optically powered CMOS circuit that decodes telemetry data and determines whether it has been addressed.**

I. INTRODUCTION

Electrical stimulation of the central nervous system (CNS) has been used as a treatment for a number of disorders [1], [2], [3]. Microelectrode arrays are used to achieve high spatial selectivity with micro-machined penetrating shanks. Caused by tethering forces from interconnects, the rigid bodies of these shanks result in chronic responses that include scarring and reduces the effectiveness of such microstimulators.

Wireless stimulators are expected to mitigate this chronic response because they have no wires to cause forces from micromotion and therefore are free to float. Some examples of wireless stimulators include addressable radio-frequency (RF) microstimulators [4], [5], [6] and an RF microstimulator array [7]. These devices receive energy and communication information from RF electromagnetic waves. This necessitates an inductive coil that limits the minimum size of the device, which is typically a cylinder with a diameter larger than 2mm. These RF stimulators are attractive for use in the peripheral nervous system, but their size limits usage in the CNS.

Photovoltaic stimulators have the ability to float, similar to RF stimulators, but they convert optical energy into electrical energy using semiconductors. Fiber guided high-efficiency III-V heterojunction photovoltaic stimulators have been used for neurostimulation [8]. Retinal photovoltaic arrays [9] exploit the two-dimensional nature of sight and utilize an image projection system to selectively activate photodiodes in an array. Additionally, gene therapy technologies have enabled photonic neurostimulation in neurons that have algal proteins [10], [11].

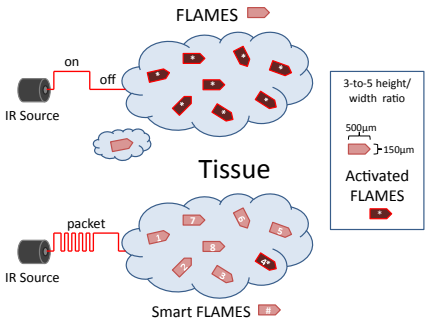

Fig. 1. Illustration of indiscriminate activation of FLAMES devices as compared to the selective activation of a Smart FLAMES device. FLAMES devices can only be selectively activated by leaving a large separation in the the tissue. The Smart FLAMES uses an optical packet to determine the specific address to activate. In this example, address four is activated.

Floating Light Activated Microelectrical Stimulators (FLAMES) with silicon photodiodes have been micromachined and tested in tissue [12]. FLAMES devices exploit the dispersive nature of white and grey matter to cause neurostimulation without a focused optical path. As seen in Fig. 1, in the original design, FLAMES devices are indiscriminately activated whenever enough optical energy is converted into electrical energy.

FLAMES with logic circuits, or Smart FLAMES, can be used to selectivity address and activate a number of disjoint neurostimulators. Compared to the original FLAMES that were indiscriminately activated, Smart FLAMES are specifically activated through a one-way communication channel that consists of an encoded optical pulse packet. This opens up an abundance of potential applications due to the large number of address selectable wireless micro-sized tissue stimulators.

II. DEVICE OPERATION

The logical operation of a Smart FLAMES follows Fig. 2. Absent any signal long enough to discharge the energy stored in the device's supply capacitance, the device enters the initial power state and requires a pulse to "wake-up".

Manuscript received March 7, 2011. This work was supported by the National Institutes of Health under Grant R01EB009100.

D. S. Freedman, and M. Selim Unlu are with the Department of Electrical Engineering, Boston University, Boston, MA 02215, USA email: dsf@bu.edu

P. S. Spuhler, E. Cevik, and M. Selim Unlu are with the Department of Biomedical Engineering, Boston University, Boston, MA 02215, USA

M. Sahin is with the Biomedical Engineering Department, New Jersey Institute of Technology, Newark, NJ 07102, USA

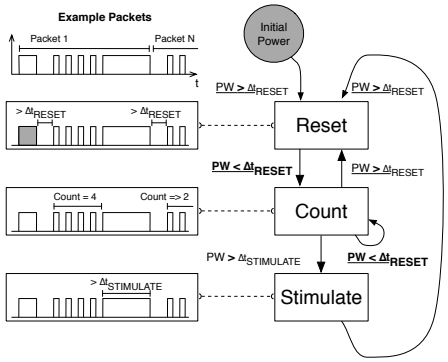

Fig. 2. Smart FLAMES state diagram for the different states as well as example waveforms of the typical optical packet. After initial powering up from either a short pulse or after a stimulate pulse, the device enters the reset state after the pulse is off for greater then t_{RESET}. After this, the device will receive a specified number of short pulses during the count state. Subsequently, a long pulse ($t_{STIMULATE}$) delivers the electric energy needed for stimulation, as illustrated in the transition from to the stimulate state. If the address ID matches the pulsed count then the output is enabled during this time. After the stimulate pulse, the device returns to the reset state and then the process is repeated.

The duration of this pulse must be at least long enough to bring the supply voltage to the expected supply voltage of approximately 1.2V-to-1.4V, which is predicted to be around 4-to-5μs from simulations.

Once the pulse is off for longer then Δt_{PACKET}, the device enters a known steady-state, the reset state. Following this should be a series of short pulses that have an off-time less then Δt_{RESET}. Each short pulse iterates a count, starting from zero, on the count block circuitry. The maximum number of independent addresses is determined by the number of count circuits that can be fit on a Smart FLAMES. After the targeted address has been pulsed the correct number of times, a long pulse will deliver the necessary charge to initiate a controlled stimulation. If the pulse is off for greater then Δt_{RESET} the device goes back to reset state and waits for the next correct sequence. If the device does not receive the correct count and long stimulate pulse, it does not attempt to do anything and will always enter the reset state after the control signal is off for Δt_{RESET}.

Because the stimululus pulse occurs shortly after the pulsing portion of the packet, the time between activation of different addresses is variable and is dependent on the address ID number. A device which is unselected will not enter the stimulate state and return to the reset state after the control signal is off for Δt_{RESET}.

III. CIRCUIT DESIGN

To decode and utilize the Smart FLAMES optical packet, the system can be divided into four functional blocks: optical power and controls, reset detection, pulse counting, and stimulation. The *optical power and controls* provides the external inputs and operating voltages needed to use the Smart FLAMES circuits. The *reset detection* and *pulse counting* stages control the functional state of the device. The *stimulation* block controls the output signal, a large voltage

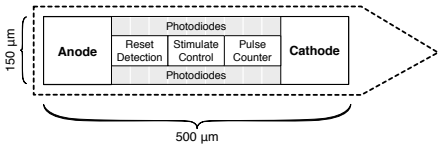

Fig. 3. Floorplan for Smart FLAMES. The anode and cathode contacts are placed on opposite ends of the device to maximize the stimulation effect in the neural tissue. The critical circuitry is enclosed in the center and contains the reset detection, stimulation control, and pulse counting blocks. The logic circuitry is surrounded by photodiodes to generate the necessary voltages for stimulation and circuit operation. The dotted outline indicates the device geometry. A pointed tip facilitates insertion into the tissue.

pulse, that is used to stimulate neural tissue. Together these functional blocks contain all the necessary circuitry to power and control the microdevice using encoded optical pulses.

The floorplan of a Smart FLAMES is shown in Fig. 3. The basic shape with anode and cathode at opposite ends of the device was studied in [13] and it was found that the voltage field in a volume conductor for any device size and current can be predicted as long as the aspect ratios are maintained; a typical aspect ratio is between three-to-five.

The photodiode power and control block consists of three sets of series photodiodes. The first is a set of photodiodes connected in series to generate the current for stimulation of the neural tissue. The second set contains two photodiodes connected in series to provide the necessary voltage to run the logic circuits. Finally, the last photodiode set contains two series photodiodes in series with a resistive load to pulse shape the input so it can be used as a control signal. The output of this pulse shaping photodiode is the input for a two-stage inverter pair/buffer that supplies the control pulse to the other functional blocks. The buffered pulses are used as inputs for the reset detection, counter, and stimulation stages.

The reset detection stage is used to reset the counter and puts the circuit and logic into a known idle state. Activation of the reset detection stage is done with an absence of a pulse for at least t_{RESET} after any length pulse. This requires rapid pulsing by the count stage to prevent the device from incorrectly returning to the reset state but advantageously allows the device to automatically reset after the end of each stimulation phase.

The counter stage consists of a finite number of count circuit elements, the number of which determines the maximum number of addressable stimulators. The counter circuit is based on CMOS dynamic logic, whereby an initial state is setup through the use of complementary reset signals that are provided by the reset detection stage.

The stimulate stage contains an original FLAMES, which is a series of photodiodes. The FLAMES device is controlled by a NAND logic gate. The two inputs to the NAND gate activate the FLAMES when the specific address is active in concert with a long positive pulse. The long pulse detector is simply two long NMOS devices, whose gates are tied to the shaped input pulse, connected in series to a capacitor. This delays the NAND gate from triggering on any short pulses,

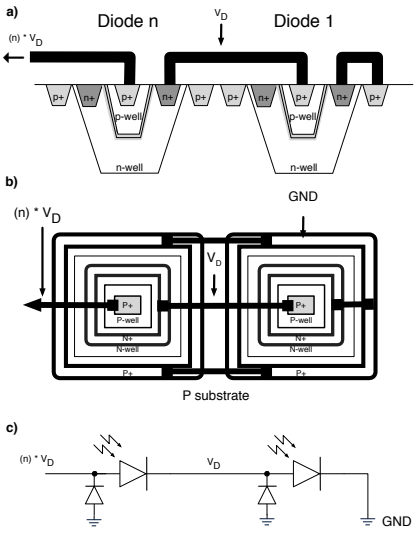

Fig. 4. Smart FLAMES photodiodes cross-sectional layout (a), overhead layout (b), and schematic view (c). The photodiodes are isolated by using triple-well technology that encloses a p-well inside an n-well. The depletion region is the shaded region in between the n-well and p-well. Additionally, the triple well causes the outer n-well to form a reverse biased pn junction diode with the p-substrate, this is illustrated in (c) where a reverse diode is connected to the anode of the photodiodes. To ensure the p-substrate does not invert, a p+ guard ring surrounds each photodiode. The reverse biased diode is covered with a higher metal layer to block it from being photoconductive.

such as the count pulse. The specific address input of the NAND gate is a connection to a specific count stage. For example, for the fourth address of a Smart FLAMES, the input would be connected to the output of the fourth count block. By design, each Smart FLAMES can only respond to one specific count, i.e. address ID.

IV. PHOTODIODES

An important design criteria for the Smart FLAMES is to be able to generate output voltages greater than what is possible with a single silicon photodiode. The high efficiency GaAs neurostimulator [8] did this through a heterogeneous tandem cell structure. Using bulk silicon processes allows for the inclusion of MOSFETs and integrated capacitors which make it possible to integrate the electronics to enable a microdevice such as a Smart FLAMES. When using standard CMOS processes, photodiodes target high efficiency n-well to p-substrate diodes that cannot be put in series. Exotic fabrication techniques can be used to fabricate silicon photodiodes in series, such as the original FLAMES devices which used silicon-on-insulator (SOI) technology and anisotropic etching to create isolated photodiodes on an oxide insulator [12].

Smart FLAMES uses a fabrication option that is available from most CMOS foundries, the triple-well, that includes an additional p-well that can be placed inside the standard n-well typically found in any CMOS process. The triple-well is typically used to make electrically insulated amplifiers by utilizing an isolated substrate. As seen in Fig. 4, series photodiodes are created with triple-wells that have an n-well inside a p-substrate. The addition of the p-well allows the diffusion layer to exist between the p-well and n-well. The n-well will be reverse-biased with respect to the p-substrate, which is kept to a low-potential through the numerous p+ contacts to ground. All device structures besides the desired p-well/n-well photodiode have a higher level metal blocking light to stop any unwanted photoconductive effects.

The Smart FLAMES uses three sets of series photodiodes whereby each can generate a voltage greater then a single photodiode. The basic structure for this is shown in Fig. 4, which can be extended to enable multiple photodiodes in series. The first photodiode (Diode 1) uses the substrate ground as the cathode voltage, with the photovoltaic voltage generated at the p+ contact. The second, and each additional diode, connects the anode from the previous diode to the cathode. The output anode will saturate at $n \times V_D$ volts with respect to the reference potential for n number of series photodiodes if each photodiode outputs V_D volts.

V. SIMULATIONS AND RESULTS

The Smart FLAMES has been designed for use with UMC's 0.18um standard triple-well process. The penetration depth of a Smart FLAMES is variable and because the amount of attenuation of near infrared (NIR) light [14], [15] has a direct effect on the amount of absorbed power from an illumination source; the Smart FLAMES device must be able to work across a large range of supply conditions. The photovoltaic response is simulated using a current source in parallel with a diode device. Current values of $10\mu A$ to 1mA were simulated to verify correction operation across a range of power using the Cadence design tools and the SPECTRE simulation engine.

As shown in Fig. 5, shortly after the initial power-on pulse, complementary reset signals are activated, causing the system to reset by setting all count circuits inactive (low). This occurs when the Smart FLAMES is operating off stored energy on the supply voltage's decoupling capacitor; during this time the supply voltage decays exponentially. After reset, the count pulses go off in order for the appropriate count stage. They activate after the high-to-low transition and then deactivate following the subsequent low-to-high transition. When the previous count value is active (high) during the positive portion of a pulse, the next count can transition and becomes the active count. The stimulus portion of the packet comes after the correct count of a targeted device. This can cause a stimulus current to be applied to the contacts of the device. After the stimulus portion of the packet transitions from high-to-low, the logic resets the device the reset state and waits for another packet or eventually dissipates any remaining energy.

VI. USAGE PARAMETERS

The feasibility of such a device must also be evaluated if this device is to be used in the CNS. The device is

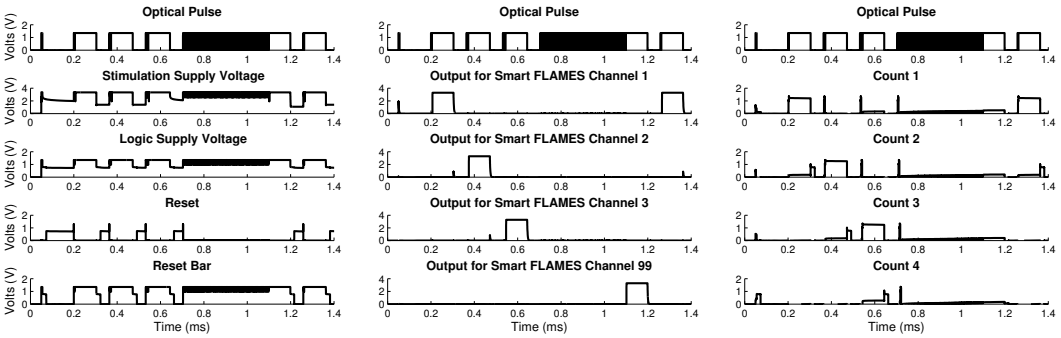

Fig. 5. Simulated response of Smart FLAMES to a wake-up pulse, followed by five packets. Packet one, two, and three target Smart FLAMES addresses one, two, and three respectively. The fourth packet activates the 99th address. The last packet activates address one again.

expected to operate at speeds consistent with neural activity, that is, a stimulation pulse every 50-to-100ms, with a $5\mu s$-to-$200\mu s$ pulse width. To maximize collection of optical energy, the photodiode surface area will occupy all available area after the control circuitry and electrode contacts have been placed. This results in a minimum surface area of $2500\mu m^2$ per photodiode. While high responsivities have been reported with standard CMOS photodiodes (0.37A/W) [16], a conservative assumption of 0.05A/W will be used when calculating the minimum required optical power. The optical penetration of NIR light in the CNS can be estimated as 10% at a distance of 1mm [14], [17], a depth comparable to similar stimulation electrodes. A worst-case assumption would be for the highest stimulation current, 1mA. This requires an optical flux of $20\frac{W}{mm^2}$; this may be prohibitively high, thus the device will need to be engineered or used at lower optical fluxes.

VII. Conclusions and Future Work

The design of a wireless electrical stimulator that receives telemetry and power from an NIR light source through a dispersive medium such a biological tissue with multiple independent addresses has been demonstrated. Challenges and solutions related to generation of stimulation voltages larger than a single photodiode have been explored. Fabrication and extraction of the Smart FLAMES from a standard die will need to be performed to be able to test Smart FLAMES in vitro. Additionally, the Smart FLAMES device will be tested in experimental animals for neural stimulation.

VIII. Acknowledgments

The authors gratefully acknowledge the contribution of the BETA laboratory at Bogizici University in Istanbul, Turkey and the LSM at EPFL in Lausanne, Switzerland.

References

[1] D. McCreery, V. Pikov, A. Lossinsky, L. Bullara, and W. Agnew, "Arrays for chronic functional microstimulation of the lumbosacral spinal cord," *Neural Systems and Rehabilitation Engineering, IEEE Transactions on*, vol. 12, no. 2, pp. 195 –207, 2004.

[2] D. C. Bradley, P. R. Troyk, J. A. Berg, M. Bak, S. Cogan, R. Erickson, C. Kufta, M. Mascaro, D. McCreery, E. M. Schmidt, V. L. Towle, and H. Xu, "Visuotopic Mapping Through a Multichannel Stimulating Implant in Primate V1," *Journal Neurophysiology*, vol. 93, no. 3, pp. 1659–1670, 2005.

[3] K. J. Otto, P. J. Rousche, and D. R. Kipke, "Cortical microstimulation in auditory cortex of rat elicits best-frequency dependent behaviors," *Journal of Neural Engineering*, vol. 2, no. 2, p. 42, 2005.

[4] G. Loeb, C. Zamin, J. Schulman, and P. Troyk, "Injectable microstimulator for functional electrical stimulation," *Medical and Biological Engineering and Computing*, vol. 29, no. 6, pp. NS13–NS19, 1991.

[5] T. Cameron, G. Loeb, R. Peck, J. Schulman, P. Strojnik, and P. Troyk, "Micromodular implants to provide electrical stimulation of paralyzed muscles and limbs," *Biomedical Engineering, IEEE Transactions on*, vol. 44, no. 9, pp. 781 –790, 1997.

[6] G. E. Loeb, R. A. Peck, W. H. Moore, and K. Hood, "BION(TM) system for distributed neural prosthetic interfaces," *Medical Engineering and Physics*, vol. 23, no. 1, pp. 9 – 18, 2001.

[7] G. Suaning and N. Lovell, "CMOS neurostimulation ASIC with 100 channels, scaleable output, and bidirectional radio-frequency telemetry," *Biomedical Engineering, IEEE Transactions on*, vol. 48, no. 2, pp. 248 –260, 2001.

[8] Y.-K. Song, J. Stein, W. R. Patterson, C. W. Bull, K. M. Davitt, M. D. Serruya, J. Zhang, A. V. Nurmikko, and J. P. Donoghue, "A microscale photovoltaic neurostimulator for fiber optic delivery of functional electrical stimulation," *Journal of Neural Engineering*, vol. 4, no. 3, p. 213, 2007.

[9] J. D. Loudin, D. M. Simanovskii, K. Vijayraghavan, C. K. Sramek, A. F. Butterwick, P. Huie, G. Y. McLean, and D. V. Palanker, "Optoelectronic retinal prosthesis: system design and performance," *Journal of Neural Engineering*, vol. 4, no. 1, p. S72, 2007.

[10] E. S. Boyden, F. Zhang, E. Bamberg, G. Nagel, and K. Deisseroth, "Millisecond-timescale, genetically targeted optical control of neural activity," *Nature Neuroscience*, vol. 8, no. 9, pp. 1263–1268, 2005.

[11] X. Han and E. S. Boyden, "Multiple-color optical activation, silencing, and desynchronization of neural activity, with single-spike temporal resolution," *PLoS ONE*, vol. 2, no. 3, p. e299, 2007.

[12] A. Abdo, V. Jayasinha, P. Spuhler, M. Unlu, and M. Sahin, "In vitro testing of floating light activated micro-electrical stimulators," in *Engineering in Medicine and Biology Society, 2009 Annual International Conference of the IEEE*, 2009, pp. 626 –629.

[13] M. Sahin and S. Ur-Rahman, "Finite element analysis of a floating microstimulator," *Neural Systems and Rehabilitation Engineering, IEEE Transactions on*, vol. 15, no. 2, pp. 227 –234, 2007.

[14] A. Abdo and M. Sahin, "NIR light penetration depth in the rat peripheral nerve and brain cortex," in *Engineering in Medicine and Biology Society, 2007 Annual International Conference of the IEEE*, 2007, pp. 1723 –1725.

[15] ——, "NIR light penetration in unfrozen samples of rat brain gray matter," in *Bioengineering Conference, 2009 IEEE Annual Northeast*, 2009, pp. 1 –2.

[16] W. Huang, Y. Liu, and Y. Hsin, "A High-Speed and High-Responsivity photodiode in standard CMOS technology," *Photonics Technology Letters, IEEE*, vol. 19, no. 4, pp. 197–199, 2007.

[17] A. N. Yaroslavsky, P. C. Schulze, I. V. Yaroslavsky, R. Schober, F. Ulrich, and H. J. Schwarzmaier, "Optical properties of selected native and coagulated human brain tissues in vitro in the visible and near infrared spectral range," *Physics in medicine and biology*, vol. 47, p. 2059, 2002.